BCSJ Award Article

2,1,3-Benzothiadiazole Dimers: Preparation, Structure, and Transannular Electronic Interactions of *syn*- and *anti*-[2.2](4,7)Benzothiadiazolophanes

Motonori Watanabe,[1,2] Kenta Goto,[1] Mamoru Fujitsuka,[3] Sachiko Tojo,[3] Tetsuro Majima,[3] and Teruo Shinmyozu*[1]

[1]Institute for Materials Chemistry and Engineering (IMCE), Kyushu University, 6-10-1 Hakozaki, Fukuoka 812-8581

[2]Department of Chemistry, Graduate School of Sciences, Kyushu University, 6-10-1 Hakozaki, Fukuoka 812-8581

[3]The Institute of Scientific and Industrial Research (SANKEN), Osaka University, 8-1 Mihogaoka, Ibaraki, Osaka 567-0047

Received March 25, 2010; E-mail: shinmyo@ms.ifoc.kyushu-u.ac.jp

The cyclophanes comprised of two 2,1,3-benzothiadiazole (BTD) rings, *anti*- and *syn*-[2.2](4,7)benzothiadiazolophanes (***anti*-1** and ***syn*-1**), were prepared for the first time. The differences of the physical properties in the overlapping mode of the π-systems are clearly observed, and ***syn*-1** shows much more significant transannular π-electronic interactions than ***anti*-1** especially in the redox properties and the stability of the radical anion species.

It is well known that charge delocalization plays an important role in material chemistry.[1] To evaluate the magnitude of the charge delocalization in bulk molecular materials, the dimeric form of aromatic rings has been often used as model compounds. The dimer radial cation has been studied as a model compound of hall transport,[2–5] but a limited number of reports on the dimer radical anion have appeared.[6] The molecules, in which two π-systems are held in a parallel fashion at a suitable transannular distance, are appropriate models for the study of the π-dimer radical anion.[7] Recently, we reported the relationship between the transannular distance of the two benzene rings and stabilization energy of the intramolecular π-dimer radical cations[8] and anions[9] of multibridged [3_n]cyclophanes ([3_n]CPs), which suggested that the stabilization energy is dependent on the transannular distance of the benzene rings in both cases and the stability of the dimer radical cation is more sensitive to the distance than the dimer radical anion.

2,1,3-Benzothiadiazole (BTD) is well known as an electron acceptor and is widely used as an electronic transportation material because of its high electron affinity.[10] BTD can be introduced to organic donor (D)–acceptor (A) molecules as an acceptor in the forms of a monomer and copolymer for OFET and OLED.[11] Although theoretical calculations predict that the *syn*-dimer of BTD with a transannular distance of 4 Å should have much larger electron coupling than the corresponding *anti*-dimer,[12] there has been no experimental data so far. *syn*- and *anti*-[2.2](4,7)Benzothiadiazolophanes are suitable models for this purpose. We report herein their structural, redox, and photophysical properties as well as radical anion species as the model of BTD dimers (Figure 1).

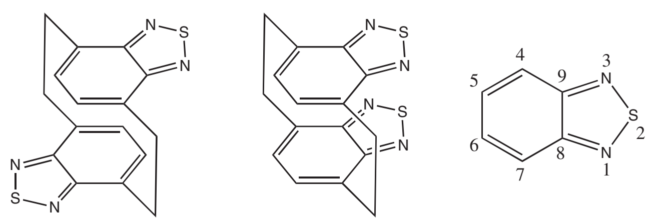

Figure 1. *anti*- and *syn*-[2.2](4,7)Benzothiadiazolophanes, ***anti*-1** and ***syn*-1**, and 2,1,3-benzothiadiazole (BTD) (**2**).

Results and Discussion

Synthesis. The BTD dimers, ***anti*-1** and ***syn*-1**, were synthesized by a method similar to that reported by Golden.[13] 4,7-Bis(chloromethyl)-2,1,3-benzothiadiazole (**3**)[14] was treated with NaI in acetone to give a pair of *syn*- and *anti*-isomers of [2.2](4,7)benzothiadiazolophane, ***anti*-1** (37%) and ***syn*-1** (9%), via a benzothiadiazole-*p*-quinodimethane intermediate followed by its dimerization.[15]

The isomers were separated by silica gel column chromatography with toluene and they are readily assigned by the chemical shift of the aromatic protons on the C-5 carbons (Ha) in the ^{1}H NMR spectrum, in which the protons (Ha) of ***anti*-1** are strongly shielded (δ 5.85) compared to the corresponding

Published on the web September 25, 2010; doi:10.1246/bcsj.20100085

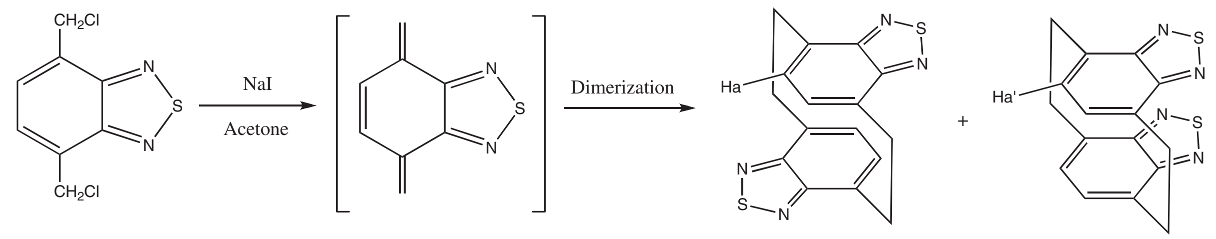

3 *anti*-1 *syn*-1

Scheme 1. Preparation of benzothiadiazole dimers, ***syn*-1** and ***anti*-1**.

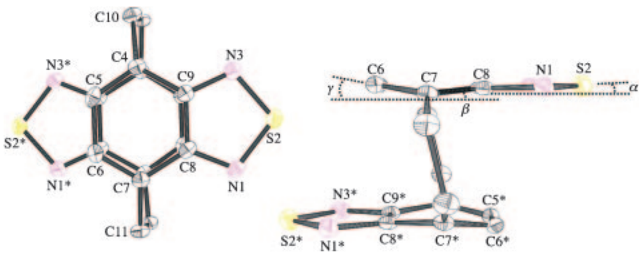

Figure 2. ORTEP drawing of the molecular structure of ***anti*-1** (−150 °C): top (a) and side (b) views. [C6–C9* 3.029 Å, C7–C4* 2.738 Å, C8–C5* 3.038 Å, ∠C9N3S2 106.45°, ∠N3S2N1 100.97°, ∠C8N1S2 106.24°, $\alpha = 3.02°$, $\beta = 7.22°$, $\gamma = 7.66°$].

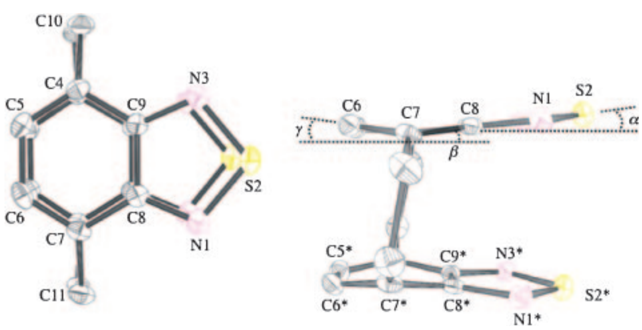

Figure 3. ORTEP drawing of the molecular structure of ***syn*-1** (−150 °C): top (a) and side (b) views. [S2–S2* 3.529 Å, N1–N1* 3.302 Å, C8–C8* 3.111 Å, C7–C7* 2.772 Å, C6–C6* 3.060 Å, ∠C9N3S2 106.68°, ∠N1S2N3 100.76°, ∠C8N1S2 106.17°, $\alpha = 4.09°$, $\beta = 7.59°$, $\gamma = 8.16°$].

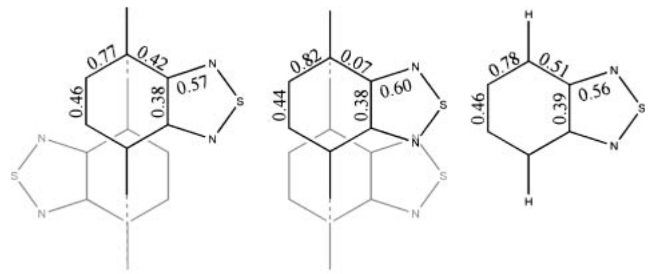

anti-1 *syn*-1 2

Figure 4. π-Bond values of ***anti*-1**, ***syn*-1**, and **2**.

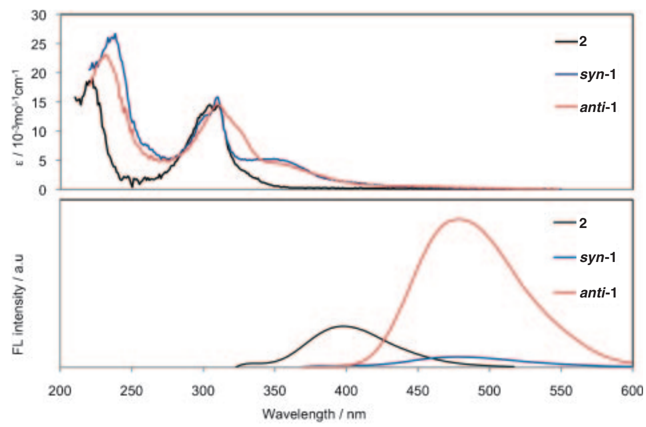

Figure 5. UV–vis and fluorescence spectra of 2,1,3-benzothiadiazole (**2**) and ***anti*-1** and ***syn*-1** in ethanol (1.0×10^{-5} M) at 293 K.

protons (Ha′) of ***syn*-1** (δ 6.81) due to the diamagnetic ring current effect of the facing aromatic ring (Scheme 1). Finally the *syn*- and *anti*-geometries were confirmed by X-ray structural analysis.

X-ray Structure. In the ORTEP drawings, the tilts ($\alpha = 3.02°$, $\beta = 7.22°$, $\gamma = 7.66°$) are observed in ***anti*-1** and the two BTD rings are held in an almost parallel orientation with the average transannular distance between the two completely overlapped six-membered rings being 2.94 Å (Figure 2). In contrast, the tilts ($\alpha = 4.09°$, $\beta = 7.59°$, $\gamma = 8.16°$) and the average transannular distance (2.98 Å) are slightly increased in ***syn*-1** (Figure 3) probably because of the repulsion between the S2–S2* atoms (3.53 Å), which are located within the van der Waals radii of the two sulfur atoms (3.70 Å).[16] Both six-membered rings of the BTD rings in ***anti*-1** and ***syn*-1** take the boat conformation due to the severe strain caused by the ethano-bridges at the *para*-positions, and the magnitude of the strain is similar to that in [2.2]paracyclophanes.[17]

BTD **2** is well known to have a quinoidal structure.[18] To compare the structures of ***anti*-1** and ***syn*-1**, the π-bond values of the BTD rings were examined (Figure 4).[19,20] The π-bond values of both isomers indicated bond alternation and therefore the quinoidal structure. The π-bond values of ***anti*-1** are comparable to those of **2**, while ***syn*-1** shows that the π-bond value of the C4–C9 bond is significantly reduced. Corresponding to this, the π-bond value of the C4–C5 bond increases to avoid sulfur–sulfur repulsion between the facing BTD rings.

UV–Vis and Fluorescence Spectra. The parent compound **2** shows two absorption bands at 222 (log $\varepsilon = 3.28$) and ca. 310 nm (log $\varepsilon = 3.15$) in ethanal (Figure 5).[21] In principle, both isomers show similar absorption spectra to that of **2**, while a new absorption band appears at ca. 350 nm both for ***anti*-1** and ***syn*-1** and these are assigned to the charge transfer (CT) bands.[22b,22c] The absorption band at ca. 222 nm in **2** shows gradual bathochromic and hyperchromic shifts in ***anti*-1** and ***syn*-1**, and this band may be assigned to the π–π interaction between the two six-membered rings in the [2.2]paracyclophane skeleton.[22a] The band at ca. 310 nm in **2** due to the BTD ring shows a slight bathochromic shift in ***anti*-1** compared to the corresponding band of ***syn*-1**.

The parent **2** exhibits a broad structureless fluorescence band at 402 nm, while the fluorescence bands appear as much broader excimer bands and show significant red shifts in ***anti*-1** (478 nm) and ***syn*-1** (479 nm) in ethanol. But the fluorescent intensity of ***syn*-1** is quite low due to the intramolecular self-quenching between the two BTD rings. The fluorescence quantum yield of ***anti*-1** (Φ 0.028) is significantly higher than those of **2** (Φ 0.005) and ***syn*-1** (Φ 0.002). No phosphorescence band was observed for both isomers in MTHF glass at 77 K.[21a]

Cyclic Voltammetric Measurements. Cyclic voltammetric measurements provide information on the intramolecular electronic interaction. The cyclic voltammograms of ***anti*-1** and ***syn*-1** along with **2** as a reference were measured versus Fc/Fc^+ in CH_2Cl_2/0.1 M Bu_4NPF_6 at a scan rate of $100\,mV\,s^{-1}$, and the profiles are shown in Figure 6 and all of the redox potentials are summarized in Table 1. The parent BTD **2** shows a reversible redox process with the halfwave reduction potential ${}^{red}E_{1/2}(I) = -1.98$ V vs. Fc/Fc^+ in CH_2Cl_2. ***anti*-1** shows a similar reversible redox process and its halfwave reduction potential [${}^{red}E_{1/2}(I) = -2.05$ V vs. Fc/Fc^+ in CH_2Cl_2] is slightly smaller than that of BTD **2**. This suggests the electronic interaction between two BTD rings is very weak in ***anti*-1**. The face-to-face orientation of the BTD rings in ***syn*-1**, on the other hand, shows distinctly separated two reversible one-electron reduction steps [${}^{red}E_{1/2}(I) = -1.92$ V and ${}^{red}E_{1/2}(II) = -1.34$ V vs. Fc/Fc^+ in CH_2Cl_2]. This indicates that ***syn*-1** significantly favors the intramolecular electronic interaction and leads to a decrease of the first reduction potential. This also suggests that ***syn*-1** can accept two electrons to generate radical anion species ***syn*-1**$^{\bullet-}$ followed by radical anion–radical anion species probably because of the more efficient π-electron delocalization over the two BTD rings in ***syn*-1** than in ***anti*-1**.

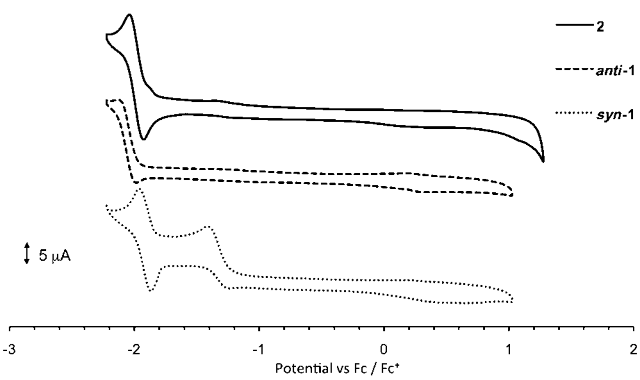

Figure 6. Cyclic voltammograms of 2,1,3-benzothiadiazole (**2**) and its dimers, ***anti*-1** and ***syn*-1**, in CH_2Cl_2/0.1 M Bu_4NPF_6 observed at a potential scan rate of $100\,mV\,s^{-1}$.

Dimer Radical Anion Formation. Formation of the dimer radical anion of the cyclophanes was examined by pulse radiolysis measurements. The ionization of DMF generates a solvated electron ($e^-{}_s$), which reacts with a substrate to give radical anion species.[23] The spectrum of the DMF solution of BTD **2** (2.5×10^{-3} M) at 50 ns after 8-ns pulse irradiation at 293 K exhibited a broad peak at ca. 600 nm that can be assigned as radical anion species. The position of this band is not affected by neither the time (50, 500, and 5000 ns) nor the concentration of **2** (from 2.5 to 20×10^{-3} M), supporting the fact that the radical anion species of **2** does not form a dimer or higher aggregation (Figures S5 and S6). Figures 7 and 8 show the transient absorption spectra of ***anti*-1** and ***syn*-1** in DMF, respectively. The radical anion species of ***anti*-1** (5×10^{-3} M), ***anti*-1**$^{\bullet-}$, shows bands at ca. 600 nm as well as a new weak and broad band at above 1600 nm (Figure 7), which can be assigned as a local excited (LE) and charge resonance (CR) bands, respectively, while the radical anion species of ***syn*-1**, ***syn*-1**$^{\bullet-}$, shows bands in shorter wavelength regions at ca. 580 and ca. 1350 nm (Figure 8). In order to observe the CR band of ***anti*-1**$^{\bullet-}$ more clearly, a γ-irradiation study was accomplished in the near-IR range.[24] Absorption spectra of ***anti*-1**$^{\bullet-}$ and ***syn*-1**$^{\bullet-}$ were measured in MTHF glassy matrix at 77 K after γ-ray radiolysis and ***anti*-1**$^{\bullet-}$ and ***syn*-1**$^{\bullet-}$ show the LE band at 576 or 538 nm as well as the CR band at 2640 or 1380 nm, respectively (Figure 9). In the multibridged [3_n]CPs, the CR bands due to the radical cation species are observed in the region of 667 ($n = 6$)–900 ($n = 2$) nm,[8] while those due to the radical anion species are in the region of 936 ($n = 5$)–1210 ($n = 2$) nm.[9] Based on these data, the bands in the near-IR region can be assigned to the dimer radical anion species of ***anti*-1** and ***syn*-1**. The stabilization energy (E_{CR})[25] of the radical anion species becomes larger as a decrease of the transannular distance (r) between the two benzene rings in multibridged [3_n]CPs and a linear relation between $\ln(E_{CR})$ and r was confirmed.[8,9] The shorter CR band of ***syn*-1**$^{\bullet-}$ (1380 nm, $E_{CR} = 43.3\,kJ\,mol^{-1}$) compared to that of ***anti*-1**$^{\bullet-}$ (2640 nm,

Table 1. Reduction Potentials in CH_2Cl_2, the λ_{max} Values of the UV–Vis (1.0×10^{-5} M) and Fluorescence Spectra (1.0×10^{-5} M) in Ethanol at 293 K, and Phosphorescence Spectra (5.0×10^{-3} M, Oxygen Free) in MTHF at 77 K

Comp.	${}^{red}E_{1/2}$/V (vs. Fc/Fc^+)	UV		FL[a)]		PL[a)]
		λ_{max}/nm	$\log\varepsilon$	λ_{max}/nm	Φ[b)]	λ_{max}/nm
2	−1.98	311, 305, 222	3.15, 3.16, 3.28	402	0.005	556
***anti*-1**	−2.05	356, 311, 233	3.64, 4.16, 4.36	478	0.028	
***syn*-1**	−1.92, −1.34	349, 310, 236	3.72, 3.20, 3.41	479	0.002	

a) $\lambda_{ex} = 311$ nm. b) Reference to anthracene (0.30).

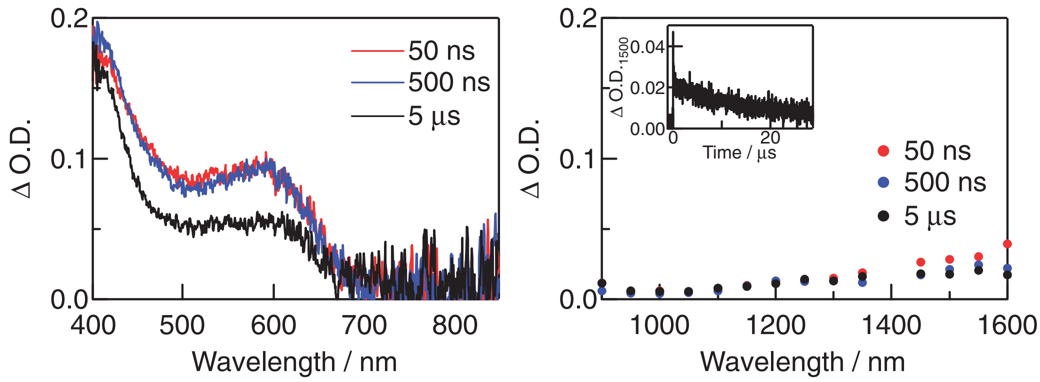

Figure 7. Transient absorption spectra obtained at 50, 500 ns, and 5 μs after 8-ns pulse irradiation during pulse radiolysis of ***anti*-1** (5 mM) in DMF under Ar at 293 K. Inset: Kinetic trace at 1500 nm during the pulse radiolysis.

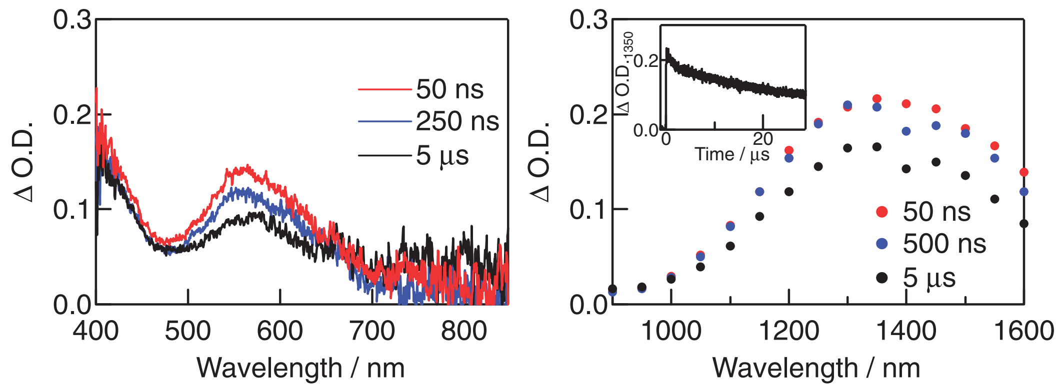

Figure 8. Transient absorption spectra obtained at 50, 250, 500 ns, and 5 μs after 8-ns pulse irradiation during pulse radiolysis of ***syn*-1** (5 mM, Ar atmosphere) in DMF at 293 K. Inset: Kinetic trace at 1350 nm during the pulse radiolysis.

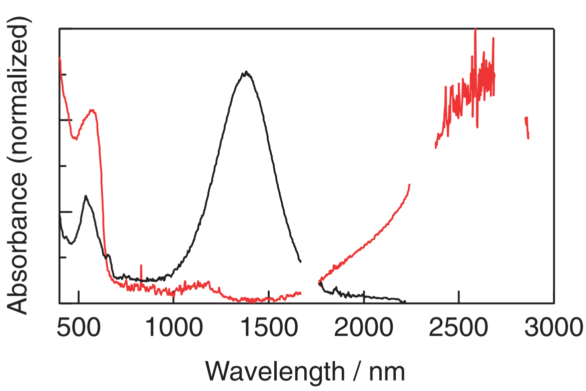

Figure 9. Absorption spectra of ***syn*-1** (black) and ***anti*-1** (red) in MTHF glassy matrix at 77 K after γ-ray radiolysis.

Table 2. Transient Absorption Spectra Obtained by Pulse Radiolysis in DMF (5 mM, Argon Atmosphere) at 293 K (λ_{max}/nm), Absorption Spectra in MTHF Glassy Matrix at 77 K after γ-Ray Radiolysis (λ_{max}/nm), and Calculated Absorption Bands with Oscillator Strengths (f) by TD-DFT Calculations

	Solvent		λ_{max}/nm	
			LE band	CR band
***anti*-1$^{\bullet-}$**	DMF		600	>1600
	glassy MTHF		576	2640
		(calcd)	543 (0.007)	1755 (0.053)
***syn*-1$^{\bullet-}$**	DMF		580	1350
	glassy MTHF		538	1380
		(calcd)	598 (0.018), 627 (0.031)	1146 (0.067)

$E_{CR} = 22.7$ kJ mol^{-1}) clearly indicates that ***syn*-1$^{\bullet-}$** is more stable than ***anti*-1$^{\bullet-}$** (Table 2). The higher stability of ***syn*-1$^{\bullet-}$** may be attributed to the shorter transannular distance between the BTD rings, as well as the complete overlap of the BTD rings. In fact, the center to center distance between the two BTD rings in ***syn*-1$^{\bullet-}$** (3.20 Å) is predicted to be shorter than that in ***anti*-1$^{\bullet-}$** (3.40 Å), while the average distance between the two six-membered rings of the BTD rings in ***syn*-1$^{\bullet-}$** (3.05 Å) is comparable to that in ***anti*-1$^{\bullet-}$** (3.00 Å) by the theoretical calculations (Gaussian 09[26] with the UB3LYP/6-311+G(d)[27] level) (Figure 10).

The CR band can be attributed to the transition from SOMO to LUMO of the radical anion species of the cyclophane, whose SOMO and LUMO orbitals may be formed by the orbital interaction between the SOMO of the radical anion of 4,7-dimethylbenzothiadiazole, **Me$_2$-BTD$^{\bullet-}$** (UB3LYP/6-311+G(d) level), and LUMO of the neutral **Me$_2$-BTD** (B3LYP/6-311+G(d)[27] level). The nodal patterns for the SOMO of ***anti*-1$^{\bullet-}$** and ***syn*-1$^{\bullet-}$** differ significantly (Figures 11 and S7). The SOMO orbital of ***syn*-1$^{\bullet-}$** has positive overlaps between the π-orbitals of the six-membered rings and the orbitals of the sulfur–sulfur atoms, whereas that of ***anti*-1**$^{\bullet-}$ has only one positive overlap between the π-orbitals of the six-membered rings, causing less transannular electronic interaction. The E_{CR} values are qualitatively estimated to be 0.10 eV for ***anti*-1**$^{\bullet-}$ and 0.57 eV for ***syn*-1**$^{\bullet-}$, respectively (UB3LYP/6-311+G(d) level). The TD-DFT calculations (UM06L/6-311+G(d,p)[28] level) suggested that ***anti*-1**$^{\bullet-}$ should show lower energy bands than ***syn*-1**$^{\bullet-}$ at near-IR region (Table 2 and Figure S8), and this result is in good agreement with the experimental results.

Conclusion

We found significant orientation effect of the transannular electronic interaction between the two BTD rings in the [2.2]paracyclophane skeleton. The anion radical species of ***syn*-1** is much more stable than that of ***anti*-1**, and ***syn*-1** can accept two electrons due to the efficient delocalization of the electrons. In the fluorescent spectra, ***syn*-1** shows self-quenching. To the best of our knowledge, this is the first example of the BTD dimer radical anion species and this result may contribute to molecular design as devices. The synthesis and transient absorption spectral measurements of the A–D and A–D–D systems comprised of the BTD ring as an acceptor are in progress and the results will be reported elsewhere.

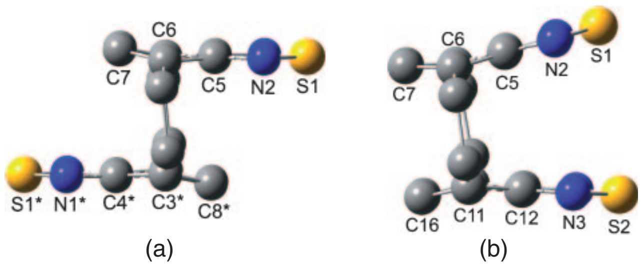

Figure 10. Center to center distances between the two BTD rings of (a) ***anti*-1**$^{\bullet-}$ (3.40 Å) and (b) ***syn*-1**$^{\bullet-}$ (3.20 Å). (UB3LYP/6-311+G(d)).

Experimental

General. IR spectra were measured as KBr pellets. The ^{1}H and ^{13}C NMR spectra were measured in $CDCl_3$. Chemical shifts are reported as δ values (ppm) relative to internal Me_4Si. The coupling constants (J) are given in hertz. Cyclic voltammetry was performed by BAS CV-50W using a cell equipped with a glassy carbon as working electrode, a platinum wire as counter electrode, and $Ag/AgNO_3$ as the reference electrode. All electrochemical measurements were performed in CH_2Cl_2 solution (5×10^{-4} mmol dm^{-3}) containing 0.10 M tetra-*n*-butylammonium hexafluorophosphate at room temperature. Elemental analyses were performed by the Service Centre of the Elementary Analysis of Organic Compounds affiliated with the Faculty of Science, Kyushu University. Analytical thin layer chromatography (TLC) was performed on Silica gel 60 F_{254} Merck. Column chromatography was performed on Kanto silica gel 60N (63–210 mm). UV–vis spectrum was performed on a HITACHI U-3500. Fluorescence and phosphorescence spectrum were performed on a HITACHI F-4500.

Pulse radiolysis was performed using an electron pulse (28 MeV, 8 ns, 0.7 kGy per pulse) from a linear accelerator at the Radiation Laboratory of ISIR, Osaka University. The probe light from a 450 W Xe-lamp (Osram, XBO-450) was detected with a multichannel spectrometer (UNISOKU TSP 601-20). The kinetic traces were estimated using a photomultiplier equipped with a monochrometer (CVI-Laser, Digikrom-240). In γ-ray irradiation experiments, samples were prepared in a Suprasil cell with a 1 or 2 mm optical path length. After freeze–pump–thaw cycle, the degassed sample was plunged into liquid nitrogen to form transparent glassy matrix, to which γ-ray from ^{60}Co source was irradiated at the Radiation Laboratory of ISIR, Osaka University. Absorption spectra were recorded using a Shimadzu UV-3100PC.

All solvents and reagents were of reagent quality, purchased commercially, and used without further purification. 4,7-

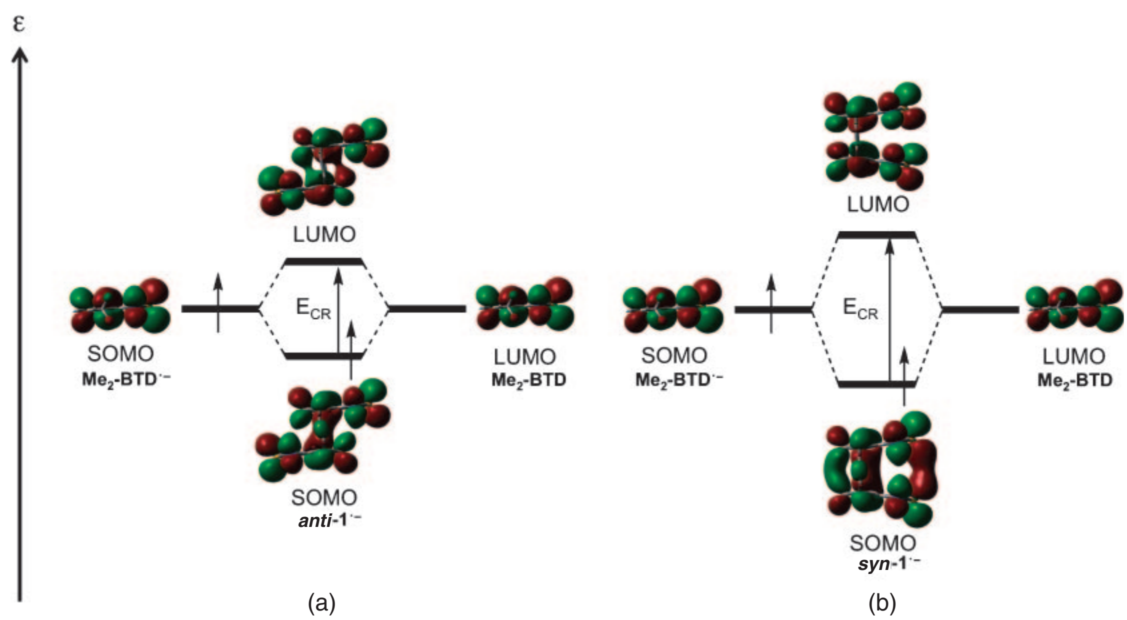

Figure 11. MO diagrams of (a) ***anti*-1**$^{\bullet-}$ and (b) ***syn*-1**$^{\bullet-}$.

Bis(chloromethyl)-2,1,3-benzothiadiazole (**3**) was synthesized according to literature procedures.[14]

***syn*- and *anti*-[2.2]Benzothiadiazolophanes.** A mixture of 4,7-bis(chloromethyl)-2,1,3-benzothiadiazole (**3**) (1.86 g, 7.98 mmol), NaI (12.0 g), and acetone (200 mL) was refluxed for 18 h with stirring. After cooling, the solvent was removed under reduced pressure and CH_2Cl_2 (200 mL) was added to the residue. The resulting precipitate was filtered and the filtrate was concentrated under reduced pressure. The concentrate was separated by silica gel column chromatography with toluene to give *anti*-isomer ***anti*-1** (473 mg, 37%, $R_f = 0.30$) and *syn*-isomer ***syn*-1** (116 mg, 9%, $R_f = 0.15$).

***anti*-1:** Pale yellow crystal (EtOH). Mp 245.0–246.5 °C; ^{1}H NMR (600 MHz, $CDCl_3$): δ 3.05–3.10 (m, 4H, CH_2), 3.73–3.79 (m, 4H, CH_2), 5.85 (s, 4H, ArH); ^{13}C NMR (100 MHz): δ 30.7, 128.3, 132.1, 157.2; IR (KBr): ν 2925 (–CH_2–) cm^{-1}; FAB-MS: $m/z = 325$ $(M + H)^+$; Anal. Calcd for $C_{16}H_{12}N_4S_2$: C, 59.23; H, 3.73; N, 17.27%. Found: C, 59.28; H, 3.77; N, 17.21%.

***syn*-1:** Yellow crystal (EtOH). Mp 220 °C (decomp.). ^{1}H NMR (600 MHz, $CDCl_3$): δ 3.31 (dd, $J = 13.1$, 4.2 Hz, 4H, CH_2), 4.16 (dd, $J = 13.1$, 4.2 Hz, 4H, CH_2), 6.81 (s, 4H, ArH); ^{13}C NMR (150 MHz): δ 31.7, 131.9, 133.7, 156.8. IR (KBr): ν 2927 (–CH_2–) cm^{-1}; FAB-MS: $m/z = 325$ $(M + H)^+$; Anal. Calcd for $C_{16}H_{12}N_4S_2$: C, 59.23; H, 3.73; N, 17.27%. Found: C, 59.47; H, 3.75; N, 17.09%.

X-ray Crystallographic Study. Measurements were made using graphite-monochromated Mo Kα ($\lambda = 0.71069$ Å) radiation and a rotating anode generator. The crystal structures were solved by direct methods, SIR97,[29] and refined by the full-matrix least-squares methods. The non-hydrogen atoms were refined anisotropically and hydrogen atoms were refined isotropically. The computations were performed using the teXsan package.[30]

***anti*-1:** Crystal color and habit are yellow and platelet, crystal dimension $0.05 \times 0.10 \times 0.10$ mm^3, formula $C_{16}H_{12}N_4S_2$, $M_r = 324.42$, monoclinic, space group $P2_1/a$ (#14), $a = 7.3666(3)$, $b = 12.6877(6)$, $c = 7.4693(3)$ Å, $\beta = 102.365(1)°$, $V = 681.93(5)$ Å^3, $Z = 2$, $D_{calcd} = 1.697$ g cm^{-1}, μ(Mo Kα) $= 3.98$ cm^{-1}, $T = 113$ K, $F(000) = 360.00$, $R = 0.057$ for 1540 observed reflections ($I > 2\sigma(I)$) and 124 variable parameters, $R_w = 0.130$ for all data, GOF = 1.74.

***syn*-1:** Crystal color and habit are yellow and platelet, crystal dimension $0.09 \times 0.22 \times 0.11$ mm^3, formula $C_{16}H_{12}N_4S_2$, $M_r = 324.42$, monoclinic, space group $P2_1/n$ (#14), $a = 7.1960(3)$, $b = 14.5419(5)$, $c = 13.0847(3)$ Å, $\beta = 95.5761(1)°$, $V = 1362.75(9)$ Å^3, $Z = 4$, $D_{calcd} = 1.581$ g cm^{-1}, μ(Mo Kα) $= 3.91$ cm^{-1}, $T = 113$ K, $F(000) = 672.00$, $R = 0.062$ for 3097 observed reflections ($I > 2\sigma(I)$) and 247 variable parameters, $R_w = 0.134$ for all data, GOF = 1.30.

Crystallographic data for the structural analyses of ***anti*-1** and ***syn*-1** have been deposited with the Cambridge Crystallographic Data Centre (CCDC) as 754964 and 754965, respectively. Copies of the data can be obtained free of charge via http://www.ccdc.cam.ac.uk/conts/retrieving.html (or from the Cambridge Crystallographic Data Centre, 12, Union Road, Cambridge, CB2 1EZ, U.K.; Fax: +44 1223 336033; e-mail: deposit@ccdc.cam.ac.uk).

Theoretical Calculations. Geometry optimization and nodal pattern of MO calculations were carried out by the DFT method at the UB3LYP/6-311+G level[27] for ***syn*-1**$^{\bullet-}$, ***anti*-1**$^{\bullet-}$ and **Me$_2$-BTD**$^{\bullet-}$ as well as B3LYP/6-311+G level[27] for **Me$_2$-BTD** using the Gaussian09[26] suite of programs, respectively. The frequency analyses were carried out for the optimized structures to give no imaginary frequency. TD-DFT calculations of ***syn*-1**$^{\bullet-}$ and ***anti*-1**$^{\bullet-}$ were carried out by UM06L/6-311+G(d,p)[28] level. The best simulated spectrum was calculated using Gaussian bands with half-band width, $\Delta 1/2$, of 1600 cm^{-1} for each transitions.

We thank the members of the Radiation Laboratory of ISIR, Osaka University for running the linear accelerator and for γ-ray radiolysis experiments. TS wishes to thank the Theme Project (Professor Tahsin J. Chow), Institute of Chemistry, Academia Sinica, Taiwan R.O.C., for the financial support of this study. TS also gratefully acknowledges the financial support by a Grant-in-Aid for Scientific Research on Innovative Areas (No. 21106015) from the Ministry of Education, Culture, Sports, Science and Technology, Japan. MW thanks the financial support by Grant-in-Aid for Academic Challenge from the Venture-Business Laboratory, Kyushu University. MW is grateful to Dr. Yuji Miyahara of Department of Chemistry, Graduate School of Sciences, Kyushu University for his kind help and discussions throughout this work. The computations were carried out using the computer facilities at the Research Institute for Information Technology, Kyushu University.

Supporting Information

The ^{1}H NMR and ^{13}C NMR spectra of ***anti*-1** and ***syn*-1**, transient absorption spectra of **2**, computational results. This material is available free of charge on the web at http://www.csj.jp/journals/bcsj/.

References

1 M. Pope, C. E. Swenberg, *Electronic Processes in Organic Crystals and Polymers*, 2nd ed., Oxford University Press, New York, **1999**.

2 B. Badger, B. Brocklehurst, *Nature* **1968**, *219*, 263.

3 a) A. Kira, M. Imamura, *J. Phys. Chem.* **1979**, *83*, 2267. b) T. Bally, K. Roth, R. Straub, *J. Am. Chem. Soc.* **1988**, *110*, 1639. c) A. Tsuchida, Y. Tsujii, S. Ito, M. Yamamoto, Y. Wada, *J. Phys. Chem.* **1989**, *93*, 1244. d) J. K. Kochi, R. Rathore, P. L. Maguères, *J. Org. Chem.* **2000**, *65*, 6826.

4 a) D.-L. Sun, S. V. Rosokha, S. V. Lindeman, J. K. Kochi, *J. Am. Chem. Soc.* **2003**, *125*, 15950. b) D. Sun, S. V. Rosokha, J. K. Kochi, *Angew. Chem., Int. Ed.* **2005**, *44*, 5133.

5 a) K. M. Knoblock, C. J. Silvestri, D. M. Collard, *J. Am. Chem. Soc.* **2006**, *128*, 13680. b) P. Bäuerle, U. Segelbacher, A. Maier, M. Mehring, *J. Am. Chem. Soc.* **1993**, *115*, 10217. c) P. Bäuerle, U. Segelbacher, K.-U. Gaudl, D. Huttenlocher, M. Mehring, *Angew. Chem., Int. Ed. Engl.* **1993**, *32*, 76.

6 a) T. Shida, S. Iwata, *J. Chem. Phys.* **1972**, *56*, 2858. b) J. Yuasa, T. Suenobu, S. Fukuzumi, *J. Am. Chem. Soc.* **2003**, *125*, 12090. c) S. V. Rosokha, J.-M. Lü, M. D. Newton, J. K. Kochi, *J. Am. Chem. Soc.* **2005**, *127*, 7411. d) V. Ganesan, S. V. Rosokha, J. K. Kochi, *J. Am. Chem. Soc.* **2003**, *125*, 2559.

7 a) F. Gerson, W. B. Martin, Jr., *J. Am. Chem. Soc.* **1969**, *91*,

1883. b) S. F. Nelsen, A. E. Konradsson, J. P. Telo, *J. Am. Chem. Soc.* **2005**, *127*, 920.

8 a) M. Fujitsuka, S. Samori, M. Hara, S. Tojo, S. Yamashiro, T. Shinmyozu, T. Majima, *J. Phys. Chem. A* **2005**, *109*, 3531. b) M. Fujitsuka, D. W. Cho, S. Tojo, S. Yamashiro, T. Shinmyozu, T. Majima, *J. Phys. Chem. A* **2006**, *110*, 5735.

9 M. Fujitsuka, S. Tojo, T. Shinmyozu, T. Majima, *Chem. Commun.* **2009**, 1553.

10 Md. Akhtaruzzaman, M. Tomura, J. Nishida, Y. Yamashita, *J. Org. Chem.* **2004**, *69*, 2953.

11 a) T. Kanbara, T. Yamamoto, *Chem. Lett.* **1993**, 419. b) A. J. Campbell, D. D. C. Bradley, *Appl. Phys. Lett.* **2001**, *79*, 2133. c) Md. Akhtaruzzaman, N. Kamata, J. Nishida, S. Ando, H. Tada, M. Tomura, Y. Yamashita, *Chem. Commun.* **2005**, 3183. d) J. Zaumseil, C. L. Donley, J.-S. Kim, R. H. Friend, H. Sirringhaus, *Adv. Mater.* **2006**, *18*, 2708. e) T. Kono, D. Kumaki, J. Nishida, T. Sakanoue, M. Kakita, H. Tada, S. Tokito, Y. Yamashita, *Chem. Mater.* **2007**, *19*, 1218. f) M. Zhang, H. N. Tsao, W. Pisula, C. Yang, A. K. Mishra, K. Müllen, *J. Am. Chem. Soc.* **2007**, *129*, 3472. g) X. Cheng, Y.-Y. Noh, J. Wang, M. Tello, J. Frisch, R.-P. Blum, A. Vollmer, J. P. Rabe, N. Koch, H. Sirringhaus, *Adv. Funct. Mater.* **2009**, *19*, 2407.

12 A. V. Vooren, J.-S. Kim, J. Cornil, *ChemPhysChem* **2008**, *9*, 989.

13 J. H. Golden, *J. Chem. Soc.* **1961**, 3471.

14 V. G. Pesin, E. K. D'yachenko, *Khim. Geterotsikl. Soedin.* **1967**, *6*, 1048.

15 a) D. J. Williams, J. M. Pearson, M. Levy, *J. Am. Chem. Soc.* **1970**, *92*, 1436. b) J. M. Pearson, H. A. Six, D. J. Williams, M. Levy, *J. Am. Chem. Soc.* **1971**, *93*, 5034.

16 L. Pauling, *The Nature of the Chemical Bond*, Cornell University Press, Ithaca, NY, **1960**, p. 260.

17 C. J. Brown, *J. Chem. Soc.* **1953**, 3265.

18 a) P. V. Luzzati, *Acta Crystallogr.* **1951**, *4*, 193. b) T. Suzuki, T. Tsuji, T. Okubo, A. Okada, Y. Obana, T. Fukushima, T. Miyashi, Y. Yamashita, *J. Org. Chem.* **2001**, *66*, 8954. c) N. M. D. Brown, P. Bladon, *Spectrochim. Acta, Part A* **1968**, *24*, 1869.

19 G. Häfelinger, *Chem. Ber.* **1970**, *103*, 2902.

20 $R/\text{Å} = 1.514 - 0.188p$ for C–C bonds and $R/\text{Å} = 1.443 - 0.167p$ for C–N bonds.

21 a) R. B. Henry, D. J. Morrison, *J. Mol. Spectrosc.* **1975**, *55*, 311. b) T. S. Lin, J. R. Braun, *Chem. Phys.* **1978**, *28*, 379.

22 a) D. J. Cram, N. L. Allinger, H. Steinberg, *J. Am. Chem. Soc.* **1954**, *76*, 6132. b) D. J. Cram, R. H. Bauer, *J. Am. Chem. Soc.* **1959**, *81*, 5971. c) M. Sheehan, D. J. Cram, *J. Am. Chem. Soc.* **1969**, *91*, 3553.

23 Pulse radiolysis of substrate in DMF is illustrated as follows.

$$\mathrm{DMF} \rightarrow \mathrm{DMF}^{\bullet+} + \mathrm{e^-}_\mathrm{s} \quad (1)$$
$$\mathrm{e^-}_\mathrm{s} + \mathrm{S} \rightarrow \mathrm{S}^{\bullet-} \quad (2)$$
$$\mathrm{DMF}^{\bullet+} + \mathrm{DMF} \rightarrow \mathrm{DMF}(-\mathrm{H}^+)^\bullet + \mathrm{DMF}(+\mathrm{H}^+)^+ \quad (3)$$

M. Fujita, A. Ishida, T. Majima, S. Takamuku, *J. Phys. Chem.* **1996**, *100*, 5382.

24 The γ-ray radiolysis of substrate in MTHF ($C_5H_{10}O$) is illustrated as follows.

$$\mathrm{C_5H_{10}O} \rightarrow \mathrm{C_5H_{10}O^{\bullet+}} + \mathrm{e^-}_\mathrm{s} \quad (1)$$
$$\mathrm{C_5H_{10}O} + \mathrm{C_5H_{10}O^{\bullet+}} \rightarrow \mathrm{C_5H_{11}O^+} + \mathrm{C_5H_9O^\bullet} \quad (2)$$
$$\mathrm{S} + \mathrm{e^-}_\mathrm{s} \rightarrow \mathrm{S}^{\bullet-} \quad (3)$$

T. Shida, *Electronic Absorption Spectra of Radical Ions*, Elsevier, Amsterdam, **1988**.

25 The stabilization energy (E_{CR}) of the dimer radical anion was estimated from the half energy of the charge resonance band.

26 M. J. Frisch, G. W. Trucks, H. B. Schlegel, G. E. Scuseria, M. A. Robb, J. R. Cheeseman, G. Scalmani, V. Barone, B. Mennucci, G. A. Petersson, H. Nakatsuji, M. Caricato, X. Li, H. P. Hratchian, A. F. Izmaylov, J. Bloino, G. Zheng, J. L. Sonnenberg, M. Hada, M. Ehara, K. Toyota, R. Fukuda, J. Hasegawa, M. Ishida, T. Nakajima, Y. Honda, O. Kitao, H. Nakai, T. Vreven, J. A. Montgomery, Jr., J. E. Peralta, F. Ogliaro, M. Bearpark, J. J. Heyd, E. Brothers, K. N. Kudin, V. N. Staroverov, R. Kobayashi, J. Normand, K. Raghavachari, A. Rendell, J. C. Burant, S. S. Iyengar, J. Tomasi, M. Cossi, N. Rega, J. M. Millam, M. Klene, J. E. Knox, J. B. Cross, V. Bakken, C. Adamo, J. Jaramillo, R. Gomperts, R. E. Stratmann, O. Yazyev, A. J. Austin, R. Cammi, C. Pomelli, J. W. Ochterski, R. L. Martin, K. Morokuma, V. G. Zakrzewski, G. A. Voth, P. Salvador, J. J. Dannenberg, S. Dapprich, A. D. Daniels, O. Farkas, J. B. Foresman, J. V. Ortiz, J. Cioslowski, D. J. Fox, *Gaussian 09 (Revision A.02)*, Gaussian, Inc., Wallingford CT, **2009**.

27 a) A. D. Becke, *J. Chem. Phys.* **1993**, *98*, 5648. b) C. Lee, W. Yang, R. G. Parr, *Phys. Rev. B* **1988**, *37*, 785. c) B. Miehlich, A. Savin, H. Stoll, H. Preuss, *Chem. Phys. Lett.* **1989**, *157*, 200.

28 Y. Zhao, D. G. Truhlar, *J. Chem. Phys.* **2006**, *125*, 194101.

29 A. Altomare, M. C. Burla, M. Camalli, G. L. Cascarano, C. Giacovazzo, A. Guagliardi, A. G. G. Moliterni, G. Polidori, R. Spagna, *J. Appl. Cryst.* **1999**, *32*, 115.

30 *teXsan: Crystal Structure Analysis Package*, Molecular Structure Corporation, **1985** and **1999**.